(4) Wang, P.; Woodward, A. E. *Macromolecules* **1987**, *20*, 2718.
(5) Tseng, S.; Herman, W.; Woodward, A. E.; Newman, B. *Macromolecules* **1982**, *15*, 338.
(6) Schilling, F. C.; Bovey, F. A; Tonelli, A. E.; Tseng, S.; Woodward, A. E. *Macromolecules* **1984**, *17*, 728.
(7) Bunn, C. W. *Proc. R. Soc. London, A* **1942**, *A180*, 40.
(8) Fisher, D. *Proc. Phys. Soc., London, Sect. B* **1953**, *B66*, 7.
(9) Meyer, K. H. *Natural and Synthetic High Polymers*; Interscience: New York, 1950.
(10) Schilling, F. C.; Bovey, F. A.; Tseng, S.; Woodward, A. E. *Macromolecules* **1983**, *16*, 808.
(11) Schilling, F. C.; Bovey, F. A.; Anandakumaran, K.; Woodward, A. E. *Macromolecules* **1985**, *18*, 2688.
(12) Tischler, F.; Woodward, A. E. *Macromolecules* **1986**, *19*, 1328.
(13) Gavish, M.; Brennan, P.; Woodward, A. E. *Macromolecules*, in press.
(14) Anandakumaran, A.; Kuo, C. C.; Mukherji, S.; Woodward, A. E. *J. Polym. Sci., Polym. Phys. Ed.* **1982**, *20*, 1669.
(15) Mukherji, S. Ph.D. Dissertation, City University of New York, New York, 1985.
(16) Cooper, W.; Vaughan, G. *Polymer* **1963**, *4*, 329.
(17) Anandakumaran, A.; Herman, W.; Woodward, A. E. *Macromolecules* **1983**, *16*, 563.
(18) Moore, W. H.; Krimm, S. *Macromol. Chem. Phys. Suppl.* **1975**, 491.
(19) Rubcic, A.; Zerbi, G. *Macromolecules* **1971**, *6*, 751.
(20) Xu, J.; Woodward, A. E. *Macromolecules* **1988**, *21*, 83.
(21) Zemel, I.; Woodward, A. E., unpublished results.

Inverse Gas Chromatography. 5. Computer Simulation of Diffusion Processes on the Column

Paul Hattam and Petr Munk*

Department of Chemistry and Center for Polymer Reserach, University of Texas at Austin, Austin, Texas 78712. *Received September 11, 1987*

ABSTRACT: The elution behavior of low molecular weight probes on IGC columns was simulated by using a computer. The IGC model was based on a polymer stationary phase of uniform thickness with a nonnegligible resistance to probe penetration. Three characteristic numbers were found to determine the whole process: Z_p characterizing the distribution of the probe between phases; Z_f describing the diffusion in the polymer phase, and Z_g related to diffusion in the gaseous phase. With Z_f vanishing or small, the elution curves differed slightly from the generally accepted ones: the appropriate correction factors were evaluated. For situations when $Z_p/Z_f < 2$, the standard evaluation procedures were virtually useless. The actual behavior of such systems was described.

Introduction

Inverse gas chromatography IGC (so-called because the material under investigation is packed on the column and a known material, probe, is injected onto the column) is a powerful investigative tool. The IGC technique has been used to study many properties of polymeric materials.[1-3]

The shape and position of the chromatographic elution curve depends on the many processes that occur on the column: diffusion of the probe in the gas phase, diffusion of the probe in the stationary phase, the partitioning of the probe between phases, adsorption of the probe on the polymer surface and on the support surface, void volume of the column, etc. Thus the elution curve contains a wealth of information, and so a method to carefully characterize it is of great importance.

We are primarily interested in the diffusion of the probe in the polymer and gas phases. In approaching this problem it would of course be desireable to describe the chromatographic process by a set of differential equations, the solution of which would yield all the required information. Unfortunately, analytical solution of such equations is very difficult-to-impossible even for the simpler chromatographic models.

Traditionally, the analysis of the peak position and shape has been performed by using either of two approaches. 1. It is tacitly assumed that chromatographic peaks, despite always being asymmetric, may be treated as symmetric Gaussian peaks, the relevant quantities being evaluated from the position of the peak maximum and from the width of the peak.[4-11] 2. The basic parameters of the system are evaluated from the moments of the elution curve.[12-14] The latter method is theoretically very elegant but suffers from an unacceptably large unreliability in the experimental measurement of the moments.

In the following, we will briefly review the traditional methods of analysis. We will then simulate the chromatographic process by using a computer and will modify the formulae utilized by traditional analysis. Mathematically, our simulation represents a numerical solution of the differential equations.

Van Deemter and co-workers[15] were among the first to analyze the shape and position of elution curves and attempt to relate these to the various column parameters and operating conditions. They used the plate theory to express the distribution of the probe on the column employing the concept of the height equivalent to one theoretical plate (HETP), H. H is essentially a measure of the separating power of the column and is related to the length of the column, L, and the total number of theoretical plates, n, as $H \equiv L/n$.

The HETP concept is applicable for elution curves which are symmetric and Gaussian in shape which allows the mathematics of statistical distributions to be utilized. In this approach, the peak parameters of interest are T_m, the elution time of the curve maximum, and $w_{1/2}$, the width of the elution curve at half its height. H_p is related to the variance of the peak, σ, by

$$H_p = L\sigma^2/T_m^2 \quad (1)$$

The subscript p denotes that the parameter is obtained from the dimensions of the elution peak. For Gaussian curves

$$w_{1/2}^2 = 8\sigma^2 \ln 2 \quad (2)$$

$$H_p = L(w_{1/2}/T_m)^2/8 \ln 2 \quad (3)$$

In broad terms the van Deemter relation for H_p may be expressed as[15]

0024-9297/88/2221-2083$01.50/0

$$H_p = A + B/u + Cu \quad (4)$$

The A term is known as the "eddy" diffusion term and was introduced by van Deemter[15] to account for the various pathways in packed columns which result in peak spreading. For an open tube with streamline flow then A would be zero. Giddings[16] has discussed the A term in greater detail.

The B term is dependent on the longitudinal diffusion of the probe in the gas phase, and the C term is a radial diffusion-related term with u being the carrier gas velocity.

Further defining these terms we may write

$$H_p = A + 2\gamma D_G/u + (C_\lambda + C_\gamma)u \quad (5)$$

where γ is a tortuosity factor (often having a value close to unity), D_G is the gaseous diffusion coefficient of the probe in the carrier gas, and C_λ and C_γ refer to contributions to H of radial diffusion of probe in liquid and gas phase, respectively. (C_λ and C_γ are often denoted as C_l and C_g in the literature, we have presented them in this manner to avoid confusion with the concentration terms in this paper.) There are many expressions for the C_γ term in the literature;[17] experimentally, on packed columns, we have found it to be negligible.[18]

According to van Deemter,[15] the C_λ term is related to the diffusion in the liquid phase as

$$C_\lambda = Kd^2k/(1 + k)^2D_L \quad (6)$$

where the distribution coefficient k is

$$k = C_L V_L/C_G V_G \quad (7)$$

V being the volume of the phase and the subscripts L and G denoting the liquid and gaseous phases. Provided that the phases are in equilibrium, C_L/C_G is the thermodynamic partition coefficient, i.e. the ratio of probe concentrations in the polymer and gas phases. D_L is the liquid diffusion coefficient of the probe in the polymer, d being the thickness of the polymer layer. K is a constant and was assigned a value of $8/\pi^2$ by van Deemter[15] though Giddings[19] has pointed out that, for a flat film of uniform thickness, K should have a value of $^2/_3$.

As mentioned above, this approach is based on the assumption that the elution curve has a Gaussian profile. For many applications of traditional gas chromatography this assumption introduces only minor errors. However, in IGC experiments the elution curve asymmetry is often severe and considerable errors can result.

In the 1960s, McQuarrie[20] realized that since a chromatographic elution curve is simply a distribution of concentration with time, then it could be fully described by its statistical moments.

The ordinary nth statistical moment M_n' is defined by

$$M_n' = \int_0^\infty C_{det}(t)t^n\,dt / \int_0^\infty C_{det}(t)\,dt \quad (8)$$

Here, C_{det} is the concentration at the detector and t is time. The central statistical moments M_n are calculated about the first ordinary moment and are given by

$$M_n = \int_0^\infty C_{det}(t)(t - M_1')^n\,dt / \int_0^\infty C_{det}(t)\,dt \quad (9)$$

The use of statistical moments in gas chromatography became popular when Kucera[21] and Kubin[22] calculated them from a mass balance equation. Many others have proceeded in a similar manner.[23-27] The theory of moments in chromatography is now firmly established.

The first ordinary statistical moment, M_1', is the center of gravity of the elution curve. In a (hypothetical) symmetrical elution curve this would be equal to T_m. The second central statistical moment, M_2, is the peak variance σ. The HETP derived from the statistical moments, H_m (the subscript m denoting a value from statistical moment analysis), may be obtained as

$$H_m \equiv LM_2/M_1'^2 \quad (10)$$

For a (hypothetical) symmetrical elution curve the values of H_m and H_p would be equal.

Because the statistical moment method is exact, it would be the preferred method of obtaining the desired quantities from elution curves. On a practical basis though, the method is plagued with difficulties and a considerable amount of literature exists on this topic.[28-33]

The problems of the moments method are connected with an extreme sensitivity of the moments to the tail of the elution curve. The effect increases fast with the order of the moment. For example, if the data collection is terminated when the signal declines to 1% of its peak value, a quite noticeable error is commited in the first moment; the second central moment and higher moments are essentially worthless. Even more damaging is any mechanism that causes extensive tailing of the elution curve, e.g., dead volume in injection chamber. In such a case, the moments may actually diverge.

On the other hand, the elution time at peak maximum, T_m, the width of the elution curve at half its height, $w_{1/2}$, and the asymmetry of the curve at half-height level are all quantities measurable with good precision. It is the goal of this paper to relate them to the basic properties of the systems studied.

Model of the Chromatographic Process

In this study, we are primarily interested in the effects of diffusion processes in the gas and polymer phases on the elution curve and its characteristics. Consequently, our model emphasizes those aspects relevant to diffusion within the chromatographic process and neglects some other experimental phenomena.

The model consists of a polymer layer of volume V_L and uniform thickness Y_L. One side of the layer is in contact with the carrier gas stream; the volume of the gas phase within the column is V_0. The diffusion coefficients of the probe in the carrier gas and polymer are D_G and D_L, respectively. The length of the column is L; the carrier gas moves through the column with a uniform velocity u. The thermodynamic equilibrium between the gas phase and the layer of polymer with a differential thickness immediately adjacent to the polymer surface is instantaneous. At equilibrium, the ratio of concentrations C_L/C_G in the two phases is equal to k. In the gas phase, there is no gradient of the probe concentration in the direction perpendicular to the streamlines. The probe is injected as an infinitely thin layer (a Dirac δ function).

The list of actual phenomena on the column, which are neglected in our model, includes (1) adsorption of the probe on the gas–polymer boundary, (2) expansion of the carrier gas along the column, (3) effects of mixing in injection and detection chambers, (4) radial diffusion in the gas phase (corresponding to C_γ term presented in introduction), and (5) any effect of eddy diffusion or of tortuosity of the carrier gas path.

Theoretical Part

Our variables are designated as follows: x, the length coordinate along the column; y, the depth coordinate within the polymer layer; t, time since probe injection; $C_G(x,t)$, concentration of probe in the gas phase; $C_L(x,y,t)$, concentration of probe in the polymer phase.

The parameters that are constants for a given IGC experiment are as follows: V_0, volume of the gas phase in the column, which is identical to the void volume; V_L, volume of the polymer phase; L, length of the column; Y_G, thickness of the gas layer; Y_L, thickness of the polymer layer; k, partition coefficient of the probe between the polymer and gas phases; D_G, diffusion coefficient of the probe in the gas phase; D_L, diffusion coefficient of the probe in the polymer; u, linear velocity of the carrier gas; m_0, the mass of injected probe.

For the partial differential equation describing the transport of the probe within the polymer we selected the one-dimensional Fickian relation

$$(\partial C_L/\partial t)_{x,y} = D_L(\partial^2 C_L/\partial y^2)_{x,t} \tag{11}$$

The transport in the gas phase is described as

$$(\partial C_G/\partial t)_x = D_G(\partial^2 C_G/\partial x^2)_t + (D_L/Y_G)(\partial C_L/\partial y)_{x,t,y=0} - u(\partial C_G/\partial x)_t \tag{12}$$

The first term on the right-hand side represents the diffusion of the probe in the gas phase; the last term is due to the flow of the carrier gas. The middle term represents the exchange of probe between the two phases: it assures the continuity of the flow within the polymer at the gas-polymer boundary.

The boundary conditions at the phase boundary and at the "bottom" of the polymer layer read, respectively

$$kC_G(x,t) = C_L(x,y = 0,t) \tag{13}$$

$$(\partial C_L/\partial y)_{x,t} = 0 \text{ for } y = Y_L \tag{14}$$

The initial conditions are

$$C_L(x,y,t = 0) = 0 \tag{15}$$

$$C_G(x,t = 0) = (m_0/V_0)\delta(x/L) \tag{16}$$

where $\delta(x/L)$ is the Dirac function.

In order to reduce the number of variables and parameters, it is convenient to introduce reduced dimensionless coordinates ζ,η; reduced time τ; and reduced dimensionless concentrations C_G^* and C_L^* as

$$\zeta \equiv x/L \tag{17}$$

$$\eta \equiv y/Y_L \tag{18}$$

$$\tau \equiv tu/L \tag{19}$$

$$C_G^* \equiv V_0 C_G/m_0 \tag{20}$$

$$C_L^* \equiv V_0 C_L/km_0 \tag{21}$$

Then the parameters will group themselves into three dimensionless expressions, Z_p, Z_g, and Z_L, defined as

$$Z_p \equiv kY_L/Y_G \equiv kV_L/V_G \tag{22}$$

$$Z_g \equiv D_G/uL \tag{23}$$

$$Z_L \equiv D_L L/uY_L^2 \tag{24}$$

The substitutions will transform eq 11–16 to

$$(\partial C_L^*/\partial \tau)_{\zeta,\eta} = Z_L(\partial^2 C_L^*/\partial \eta^2)_{\zeta,\tau} \tag{25}$$

$$(\partial C_G^*/\partial \tau)_\zeta = Z_g(\partial^2 C_G^*/\partial \zeta^2)_\tau + Z_L Z_P(\partial C_L^*/\partial \eta)_{\zeta,\tau,\eta=0} - (\partial C_G^*/\partial \zeta)_\tau \tag{26}$$

$$C_G^*(\zeta,\tau) = C_L^*(\zeta,\eta = 0,\tau) \tag{27}$$

$$C_L^*(\zeta,\eta,\tau = 0) = 0 \tag{28}$$

$$C_G^*(\zeta,\tau = 0) = \delta(\zeta) \tag{29}$$

$$(\partial C_L^*/\partial \eta)_{\zeta,\tau}(\zeta,\eta = 1,\tau) = 0 \tag{30}$$

Before continuing with the analysis, we need to address a special case of a probe that equilibrates instantly with the polymer phase. Instant equilibration may be described by values of D_L and Z_L equal to infinity. Simultaneously, the derivative $(\partial C_L/\partial y)_{x,t}$ and related derivatives become equal to zero and our transport equations are indetermined.

In this situation

$$kC_G(x,t) = C_L(x,y,t) \tag{31}$$

and the middle term of the transport eq 12 must be replaced by $-(kY_L/Y_G)(\partial C_G/\partial t)_x$. Then the set of eq 25–30 may be replaced by a simpler one

$$(\partial C_G^*/\partial \tau)_\zeta = [Z_g(\partial C_G^*/\partial \zeta^2)_\tau - (\partial C_G^*/\partial \zeta)_\tau]/(1 + Z_p) \tag{32}$$

$$C_G^*(\zeta,\tau = 0) = \delta(\zeta)/(1 + Z_p) \tag{33}$$

The experimentally accessible quantity is the probe concentration at the detector, $C_{det}(t)$, which may be equated with $C_G(x = L,t)$.

Our computer simulation consists of replacing the differential equations by difference equations and of following the time development of concentrations within both the gas and polymer phases as well as at the column outlet.

For this purpose, we have divided the column into N_C compartments along the column length. Similarly, the film of polymer is divided into N_L layers. At the start of the simulation, a unit amount of probe is introduced into the gaseous part of the first compartment. Then, the progress of the chromatographic process is simulated as a sequence of alternating diffusion and flow transport steps. The flow steps consist simply of shifting the contents of each gaseous compartment into the following one. This step corresponds to the third term in eq 26. Each flow step is followed by a series of at least three diffusion cycles. Each diffusion cycle includes the diffusion of the probe along the column (first term of eq 26) and the diffusion in the y direction (eq 25 and the second term of eq 26). When simulating diffusion, it is important to select the individual transport steps small enough in order to preserve the validity of the difference algebra. Accordingly, we have designed our diffusion transfers in such a way that the transport across any boundary was always small enough to reduce the difference of concentrations on both sides of the boundary (i.e., in the neighboring layers or compartments) by not more than 20%. This strategy often necessitated an increase of number of diffusion cycles per flow step to values greater than three. In addition, it was often also necessary to simulate the diffusion steps across the phase boundary (second term of eq 25) by several smaller steps. The number of needed diffusion steps was steeply increasing with increasing values of the parameters Z_p and $1/Z_L$.

The algorithm for simulating the limiting case of instantaneous equilibration ($Z_L \to \infty$) was, of course, much simpler: the diffusion in the y direction was replaced by partitioning of the probe between the gas and polymer compartments.

The dependence of the probe concentration at the column outlet on the number of flow steps was considered as a representation of the chromatographic elution curve, which was further analyzed by standard means as will be presented in results and discussion.

The results obviously depended on the arbitrarily selected values N_C and N_L. To remove this dependency, we have repeated the simulation for several values of N_C and N_L and extrapolated them to infinite values of these parameters (i.e., toward $1/N_C$ and $1/N_L$ approaching zero).

Under most circumstances, it was possible to obtain reliable extrapolated values from N_C values ranging between 100 and 300. The calculations were much less sensitive toward N_L values. With $N_L = 3$ usually giving acceptable values, the range of $N_L = 3$–10 was always fully satisfactory. Nevertheless, the necessity to extrapolate the computer data led to some residual uncertainty, which caused minor scatter in our results. However, we will demonstrate that this scatter does not compromise the validity of our results.

Results and Discussion

It is apparent from the transport eq 25 and 26 that the reduced probe elution curve $C_{det}^*(\tau) \equiv C_{det}(t)V_0/m_0$ depends only on the three chromatographic parameters Z_g, Z_p, and Z_L; and so do all the quantities derived from the elution curve. Conversely, the maximum information we may extract from the elution curve are the values of these three parameters. We would need auxiliary information in order to be able to convert these parameters into their constituent variables.

We have characterized our simulated elution curves by a number of (mutually interdependent) parameters: $\mu_1' \equiv \int \tau C_{det}^*(\tau)\, d\tau$, the first reduced moment of the elution curve; $\mu_2 \equiv \int (\tau - \mu_1')^2 C_{det}^*(\tau)\, d\tau$, the second central reduced moment of the curve; $n_m \equiv n_1'^2/n_2$, number of theoretical plates from the moment analysis; τ_{max}, reduced time for maximum of the curve; $w_{1/2}$, width of the elution curve at the half-height in reduced time units; $f_{1/2}$, the front half-width of the curve (up to τ_{max}); $b_{1/2} \equiv w_{1/2} - f_{1/2}$, the back half-width; $r_{1/2} \equiv f_{1/2}/b_{1/2}$, ratio of the half-widths; $n_p \equiv 8 \ln 2/(w_{1/2}/\tau_{max})^2$, number of theoretical plates from curve shape analysis.

Before presenting the dependences of our parameters on Z_g, Z_p, and Z_L, we need to recast the results of the traditional approach in the terms of our reduced parameters. The predicted shape of the peak is Gaussian both on the column and at the detector no matter what the values of Z_g, Z_p, and Z_L. That implies that $r_{1/2} = 1$. Further, it is routinely assumed that

$$\mu_1' = \tau_{max} = 1 + Z_p \tag{34}$$

Van Deemter's theory and the moments theory predict for the number of theoretical plates

$$1/n_m = 1/n_p = 2Z_g + KZ_p/Z_L(1 + Z_p)^2 \tag{35}$$

where the constant K equals $8/\pi^2$ according to van Deemter and $^2/_3$ according to Giddings.[19]

When analyzing the dependence of the chromatographic results on the determining parameters, it is convenient to use instead of Z_L its inverse $Z_f \equiv 1/Z_L$. The parameter Z_f is more appropriate for description of deviations of the result from the limiting case of instantaneous equilibrium. For example, eq 35 now adopts a more pleasing form

$$1/n_m = 1/n_p = 2Z_g + KZ_fZ_p/(1 + Z_p)^2 \tag{36}$$

Let us present first the results for the computations using moments of the curve. Irrespective of the values of Z_g, Z_p, Z_f, both μ_1', and n_m satisfied eq 34 and 36 within 0.1%. Even this tiny error is probably a result of our extrapolation procedure with respect to the computer parameters N_C and N_L. The value of K was found to be 0.7, slightly higher than $^2/_3$ predicted by Giddings.[19] Besides confirming the soundness of the method of moments, the above results served also to reassure us of the soundness of our computational procedure.

We have already explained that despite their theoretical superiority, the moments of the elution curve have little practical significance because their measurement is subject to an unacceptably large experimental error. In practice, the analysis of the elution curve must be based on its shape and on the position of its maximum, its width, and its asymmetry: these quantities are usually measureable with very good precision.

We will first present the results for the case of instantaneous equilibrium ($Z_f = 0$). In this case, the concentration profile of the probe along the column at any given time before the band is eluted remains Gaussian for all values of Z_g and Z_p. The width of the band increases with the progress of the elution as expected. However, the elution curve C_{det}^* vs τ is asymmetric. This should not be surprising: each point on the elution curve represents a sampling of column concentration profile at the column outlet at different times while the width of the peak (on the column) is continuously increasing during the time when the band is passing through the sampling point (detector). We have found that the ratio of the half-widths and reduced elution time may be described by the following relations valid for all values of Z_p

$$r_{1/2} = 1 - (1.664\sqrt{Z_g} + 1.225Z_g) \tag{37}$$

$$\tau_{max} = (1 + Z_p)(1 - 2.77Z_g) \tag{38}$$

For example, when methane (used as a marker) is studied on a 50-cm column at about 16 mL/min flow rate at 80 °C with nitrogen as the carrier gas, Z_g is found to be approximately 0.003. In this case we calculate $r_{1/2} = 0.912$ and $\tau_{max} = 0.992$. Thus, the assymmetry of the peak is already significant. Identifying τ_{max} with $(1 + Z_p)$ thus leads to an error in measurement of the elution volume of about 1%: this error is, however, systematic because the retention volumes of the other probes are always calculated by assuming that the elution volume of marker is equal to the void volume of the column.

For the number of theoretical plates we have found in full agreement with van Deemter theory

$$1/n_p = 2Z_g \text{ for } Z_f = 0 \tag{39}$$

Hence, for the case of instantaneous equilibrium, the width of the peak may be analyzed in the traditional way.

Simulation of chromatographic processes with slow probe transfer ($Z_f > 0$) yielded much more complicated results. We have found that in this case the progress of the probe along the column has two distinctly different time periods. In the first one, the injected probe remains essentially in the gas phase and penetrates only very slowly into the polymer. This time interval is best characterized by the fact that the ratio of the masses of the probe in the polymer and gas phases is much less than Z_p (it would be equal to Z_p if the equilibration were instantaneous). As the time progresses, the ratio will approach Z_p and remain there for the rest of the experiment. This observation refers to the ratio of masses on the *whole* column: locally the two phases are *not* in equilibrium. In the front part of the peak, the probe is mainly in the gas phase and in the back part, is mainly in the polymer.

The nature of the elution curve is determined by the relation of the time needed for elution of the probe to the time needed for the approximate equilibration in the above mentioned sense. If the probe reaches the outlet of the column before it can appreciably penetrate into the polymer, its elution behavior will be similar to that of the marker. If it spends enough time on the column, it will progress along the column as a more or less Gaussian band with a retention time corresponding to its Z_p value. Of course, between these two time periods must exist a transition region, where the overall behavior is rather

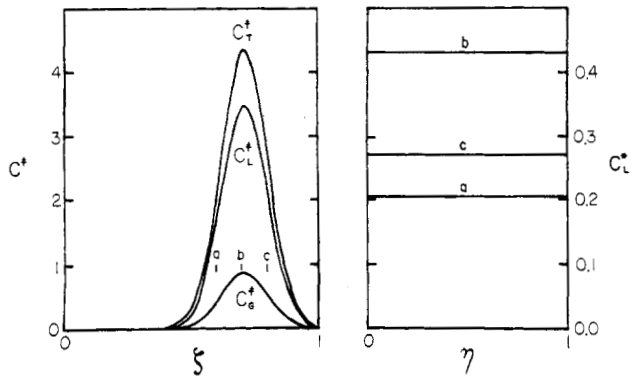

Figure 1. Distribution of the probe on the column when 0.1% of probe has been eluted, case of instantaneous equilibration: $Z_f = 0$, $Z_p = 4$, and $Z_g = 0.002$. Left-hand side: dependence of the average concentrations C^* on the reduced length ζ. Right-hand side: dependence of the reduced concentration C_L^* on the reduced depth η. Curves labeled a, b, c, and d refer to the positions marked similarly on the left-hand side.

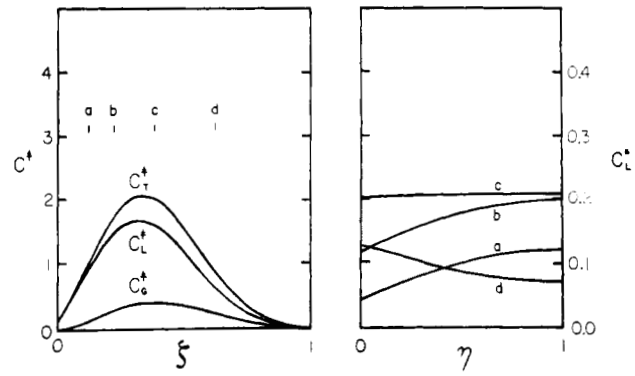

Figure 2. Distribution of the probe on the column when 0.1% of probe has been eluted, case of pseudoequilibrium: $Z_f = 1.0$, $Z_p = 4.0$, and $Z_g = 0.002$. The same dependences as in Figure 1.

complex. We have found that the ratio Z_p/Z_f determines the type of situation applicable to the experiments. The most anomalous behavior is found for $Z_p/Z_f = 1$; when $Z_p/Z_f > 2$, the pseudoequilibrium regime is reached, while $Z_p/Z_f < 0.5$ produces a relatively sharp peak but with a long low tail. This behavior we will call marker-like behavior.

The distribution of the probe within the column is depicted by Figures 1–4. All these figures show the probe concentration at the moment when the front edge of the probe band reaches the detector (more precisely, when 0.1% of the probe has been eluted).

For the presentation of our results we have introduced a number of new parameters: $C_L^*(\zeta)$, the position-dependent average-reduced concentration in the liquid phase. The corresponding quantity for the gaseous phase, $C_G^*(\zeta)$, is of course identical with C_G^*. The sum of these two parameters we have denoted as C_T^*. Furthermore we have introduced C_L°, the total reduced mass in the liquid phase, and C_G°, the total reduced mass in the gaseous phase. (Of course the sum $C_L^\circ + C_G^\circ$ represents the reduced mass remaining on the column.)

Equations to define these new parameters are

$$C_L^*(\zeta) \equiv \int_0^1 C_L^*(\zeta,\eta)\, d\eta \tag{40}$$

$$C_L^\circ \equiv \int_0^1 C_L^*\, d\zeta \equiv \int_0^1 \int_0^1 C_L^*(\zeta,\eta)\, d\zeta\, d\eta \tag{41}$$

$$C_G^\circ = \int_0^1 C_G^*\, d\zeta \tag{42}$$

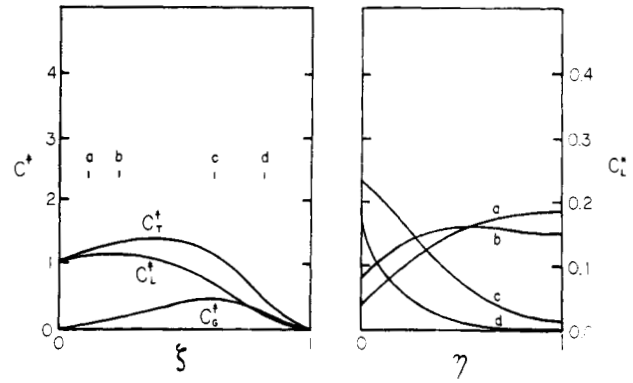

Figure 3. Distribution of the probe on the column when 0.1% of probe has been eluted, case of the transition region: $Z_f = 4.0$, $Z_p = 4.0$, and $Z_g = 0.002$. The same dependences as in Figure 1.

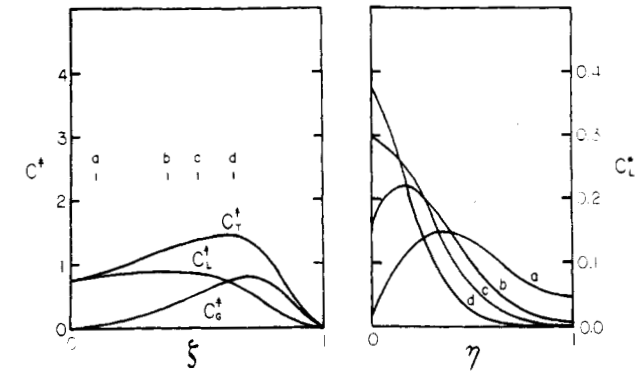

Figure 4. Distribution of the probe on the column when 0.1% of probe has been eluted, case of marker-like behavior: $Z_f = 10$, $Z_p = 4$, and $Z_g = 0.002$. The same dependences as in Figure 1.

On the left-hand side of Figures 1–4, the position-dependent average-reduced concentrations in the gas phase, polymer phase, and their sum (C_G^*, C_L^*, and C_T^*, respectively) are plotted vs the reduced length coordinate (ζ). On the right-hand side of the figures, the reduced concentration of the probe (C_L^*) is plotted as a function of the reduced depth coordinate (η) at several positions (i.e. ζ values) within the probe band. For all figures, $Z_g = 0.002$ and $Z_p = 4.0$ were selected. The values of Z_f were 0.0, 1.0, 4.0, and 10.0. These values correspond to chromatographic behavior of systems in the region of instantaneous equilibration, in the region of pseudoequilibration, the transition region, and the marker-like region.

Figure 1 illustrates instantaneous equilibration and shows that the distribution of the probe on the column is quite symmetrical with, of course, the probe evenly distributed throughout the depth of the polymer. In Figure 2, we show the region of pseudoequilibrium; the curves are becoming broader and asymmetric. The distribution of the probe within the polymer is nonlinear but close to the peak maxima the probe is quite evenly distributed. Figure 3 represents the transition region. The concentration profiles have become very asymmetric. The dependence of C_L^* on ζ has an almost constant value within the rear portion of the probe band. C_L^* sharply decreases toward the bottom of the polymer layer in the front portion of the eluting band; the reverse is true in the back portion.

Figure 4 represents the marker-like behavior. The probe band progresses fast along the column and remains relatively sharp (its sharpness is increasing with increasing Z_p/Z_f ratio). Behind the probe band in the mobile phase, the average concentration in the stationary phase is almost constant. The very slow decrease of C_L^* behind the probe

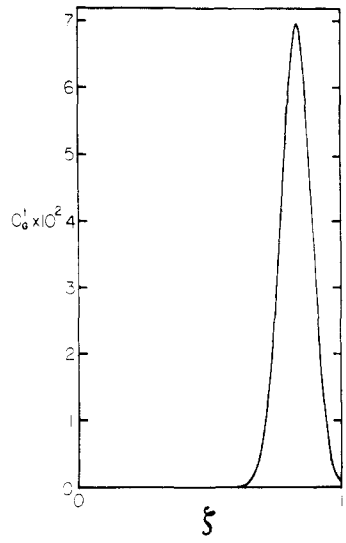

Figure 5. Distribution of the probe on the column when 0.1% of probe has been eluted, case of gaseous diffusion only: $Z_f = 0$, $Z_p = 0$, and $Z_g = 0.002$. Dependence of the average concentration in the gas phase C_G^* on the reduced length ζ.

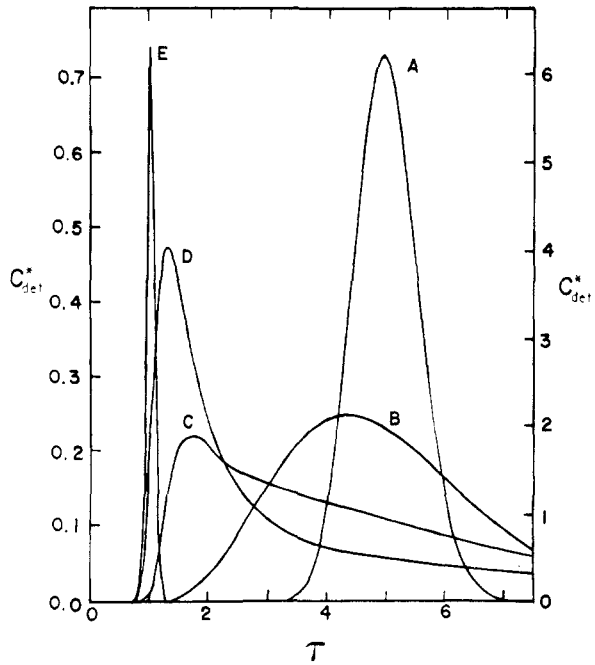

Figure 6. Dependence of the reduced concentration at the detector C_{det}^* on the reduced time τ. Curves A–E correspond to the conditions for Figures 1–5, respectively. Left-hand axis applies to curves A–D; right-hand axis applies to curve E.

band reflects the fact that the probe, which entered the polymer, will elute from it very slowly; this will eventually lead to an extended tail on the elution curve.

The concentration profiles in the polymer are very complex. A passing probe band creates a high concentration close to the phase boundary. However, before the probe can diffuse toward the bottom, the probe band is gone and the probe starts diffusing out of the polymer phase. The result is a profile with a prominent maximum.

In Figure 5 we have presented the case of purely gaseous diffusion ($Z_f = 0$, $Z_p = 0$). As expected the distribution of probe in the gas phase results in a quite symmetrical peak. (Of course the same behavior would be observed if $Z_f = \infty$ regardless of the value of Z_p).

Figure 6 gives a clearer picture of the effect of the various conditions on the resultant elution curves. The

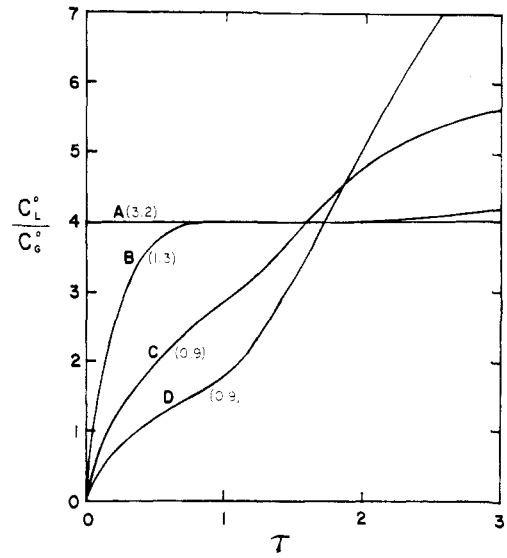

Figure 7. Dependence of the average reduced concentration ratio C_L°/C_G° on the reduced time τ. Curves A–D correspond to the conditions for Figures 1–4, respectively. Numbers in parentheses refer to the time at which probe begins to elute from the column.

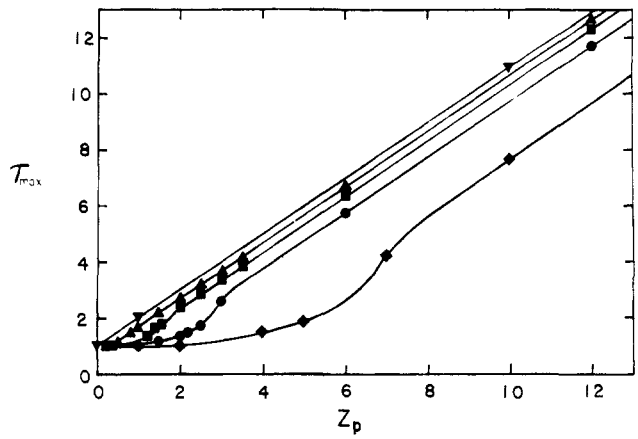

Figure 8. Dependence of the reduced time at peak maximum τ_{max} on Z_p at several values of Z_f. Selected values of Z_f: (♦) 5.0; (●) 2.0; (■) 1.0; (▲) 0.5; (▼) 0.

elution curves labeled A–E correspond to the conditions for Figures 1–5.

In Figure 7 we have presented the dependence of the reduced concentration ratio (C_L°/C_G°) on the reduced time coordinate (τ). When the system is at equilibrium, the concentration ratio equals Z_p (which in this case is 4). The numbers in parentheses in the figure show the time at which probe began to elute from the column.

As expected, for instantaneous equilibration the concentration ratio equals Z_p at all times. Of course for other conditions as the probe is eluted from the column the dependence of C_L°/C_G° on τ changes. In the case of pseudoequilibrium the concentration ratio rapidly attains a value equal to Z_p and maintains this value until the probe begins to elute. In the transition region the concentration ratio shows a gradual increase with time until elution begins, at which point the concentration ratio rises less sharply with time and begins to level off somewhat above the equilibrium value of 4. For marker-like behavior the concentration ratio again shows a gradual increase with time (though less than for the transition region), until the probe begins to elute. At elution the concentration ratio begins to increase rapidly with time.

The preceding figures have been concerned with the distribution of the probe on the column. We will now

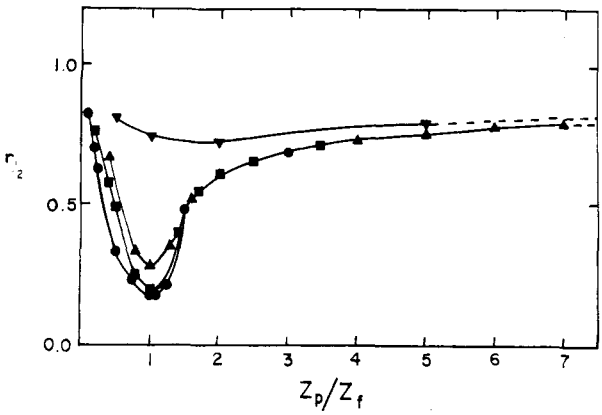

Figure 9. Dependence of the ratio of half-widths $r_{1/2}$ on the ratio Z_p/Z_f at $Z_g = 0.002$ and at selected values of Z_f: (●) 2.0; (■) 1.0; (▲) 0.5; (▼) 0.1.

examine various characteristics of the elution curves.

In Figure 8 we present the dependence of the reduced time at peak maximum (τ_{max}) on Z_p, for several values Z_f. (For clarity only selected points are presented on this plot.) From the data we were able to obtain two relationships for τ_{max} within certain ranges of the ratio Z_p/Z_f.

$$Z_p/Z_f > 1.3$$

$$\tau_{max} = (1 + Z_p)(1 - 2.77Z_g) - 0.482Z_f(1 + 0.68Z_f/Z_p) \quad (43)$$

$$Z_p/Z_f < 0.8$$

$$\tau_{max} = (1 - 2.77Z_g) + (Z_p/2Z_f)^2 \quad (44)$$

Equation 43 typifies the region of pseudoequilibrium while eq 44 represents the marker-like region. For eq 43, in the worst case the discrepancy was ±2% (near to $Z_p/Z_f = 1.3$) which decreased to a negligible difference as Z_p/Z_f approached 20. For eq 44 the discrepancy was ±4% for the worst case, again decreasing to negligible difference as Z_p/Z_f approached zero.

We next examined the asymmetry of the elution curves through use of the ratio of half-widths ($r_{1/2}$). Figure 9 illustrates the dependence of $r_{1/2}$ on the ratio Z_p/Z_f. Although the dependence is rather complex, as one increases the value of Z_f, there is an approach to a universal curve. With increase in the ratio Z_p/Z_f the curve reaches a limiting value of 0.85.

Our next step was to investigate the van Deemter type analysis. In Figure 10 we show the dependence of $1/n_p$ on $Z_p/(1 + Z_p)^2$, and in Figure 11 we show the reduced van Deemter plot: the dependence of $1/n_p$ on $Z_fZ_p/(1 + Z_p)^2$. In both cases the broken lines are the predicted van Deemter lines. The reduced van Deemter plot (Figure 11) gives a much clearer picture of the dependence. The arrows on the plot show increasing values of Z_p, the plots possessing a triangular shape. At the base of the triangle is the region of "marker-like" behavior, the steep rise being the transition region and the third side being the region of pseudoequilibrium. It is easily seen that the van Deemter approach is valid only at high values of the ratio Z_p/Z_f. The reduced plot allowed us to obtain an expression for $1/n_p$ in the region of pseudoequilibrium:

$$1/n_p = 2Z_g + 0.7Z_fZ_p/(1 + Z_p)^2 + 0.965[Z_fZ_p/(1 + Z_p)^2]^2 \quad (45)$$

Equation 45 is the van Deemter equation extended by a correction factor of $0.965[Z_fZ_p/(1 + Z_p)^2]^2$.

A potentially useful expression was obtained from our investigation of the back half-width, $b_{1/2}$. The dependence

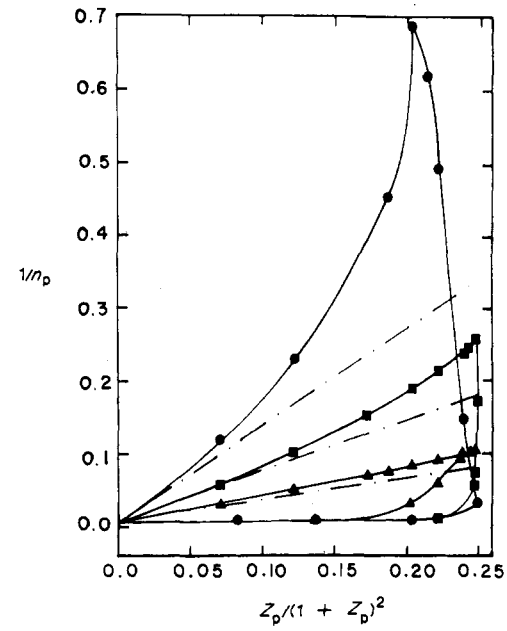

Figure 10. Van Deemter plot showing the dependence of the inverse number of theoretical plates determined from peak parameters, $1/n_p$ on $Z_p/(1 + Z_p)^2$ at selected values of Z_f: (●) 2.0; (■) 1.0; (▲) 0.5; (▼) 0.1. Broken lines correspond to the predicted van Deemter lines based on $K = {}^2/_3$ (see eq 36).

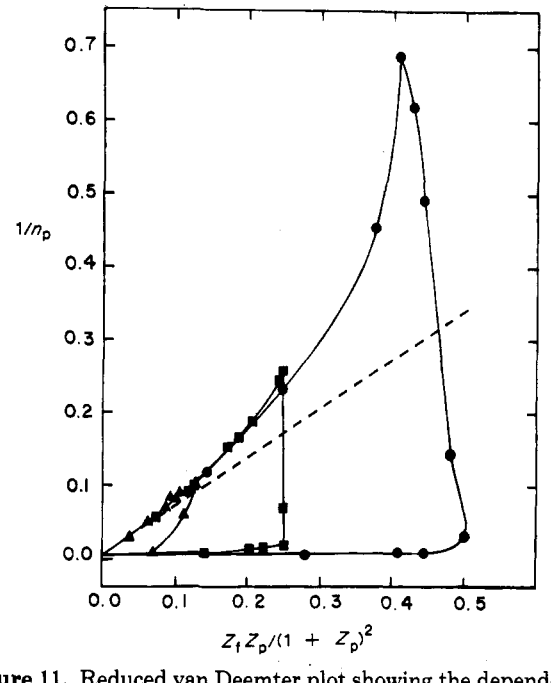

Figure 11. Reduced van Deemter plot showing the dependence of $1/n_p$ on $Z_fZ_p/(1 + Z_p)^2$ for selected values of Z_f: (●) 2.0; (■) 1.0; (▲) 0.5. Broken line corresponds to the predicted reduced van Deemter line based on $K = {}^2/_3$ (see eq 36).

of $b_{1/2}{}^2$ on the product Z_fZ_p is illustrated in Figure 12. For the region of pseudoequilibrium we determined that

$$b_{1/2}{}^2 = 1.22Z_fZ_p \quad (46)$$

In the worst cases the discrepancy between calculated and actual values were ±5%. Analysis of the front half-width, $f_{1/2}$, has at present not produced any potentially useful expressions.

Conclusions

Our computer simulation method reproduced faithfully the results of the only theory which is capable to describe

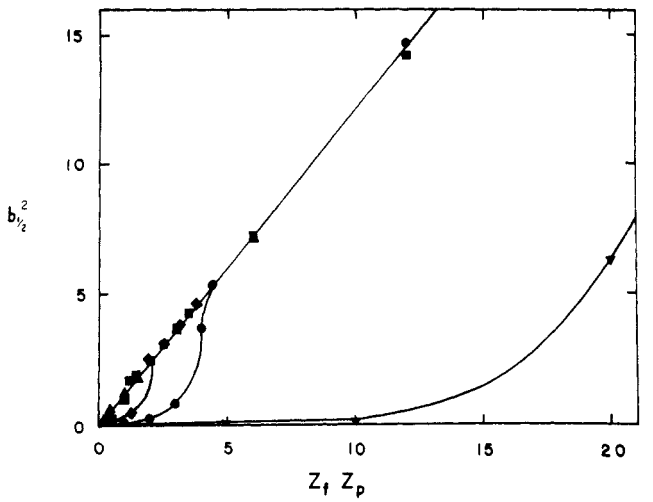

Figure 12. Dependence of $b_{1/2}^2$ on the product Z_fZ_p for selected values of Z_f: (●) 5.0; (■) 2.0; (◆) 1.0; (▲) 0.5; (▼) 0.1.

the chromatographic elution curves rigorously—namely, the theory of moments. This proves the soundness of our computational procedures.

On the other hand, our results illuminated clearly the shortcomings of the routine procedures of extracting physicochemical data from the position and shape of the elution peaks. We were able to distinguish four different regimes on the column.

1. When the probe equilibrates instantaneously throughout the polymer, the position of the peak reflects the distribution coefficient for the probe. However, a small but not negligible correction must be applied to the values evaluated in a traditional way. Our simulation predicts that the elution bands are asymmetric even in this case of instantaneous equilibrium.

2. When the characteristic ratio Z_f/Z_p remains small, the probe distributes itself between the phases in more or less equilibrium manner. In this pseudoequilibrium situation, it is still possible to extract the distribution coefficient from the peak position, and the diffusion-related quantities from the peak width. However, the necessary corrections to the traditional formulae become more significant.

3. In a transition region where $Z_f/Z_p \approx 1$, the elution curves become very asymmetric. The traditional parameters of peak position, peak width and peak asymmetry become of little value for obtaining the basic characteristics of the probe–polymer system.

4. Finally, in the marker-like region when $Z_f \gg Z_p$, the probes elute essentially as soon as the marker does. The elution peaks are very narrow, and even their asymmetry at the half-height level is only moderate. The probe polymer interaction in this case is manifested only in the tail of the curve, which becomes lower and lower as the ratio Z_f/Z_p is increasing. It may be noted that our elution peaks in this region resemble experimental peaks observed for polymers close to their glass transition temperature. These experimentally obtained peak shapes have traditionally been interpreted as being due to surface retention.

Evaluation of IGC experiments that fall into the transition or marker-like region is impossible by the traditional means. In order to extract the basic chromatographic quantities from the elution curves, we would need to characterize them by some new parameters that would weigh more heavily the tails of the peaks. We plan to do so in our future research.

Acknowledgment. We are grateful for the financial support of the National Science Foundation (Grant No. DMR-8414575) and the National Aeronautics and Space Administration (Grant No. NAG 9-198).

References and Notes

(1) Laub, J. R.; Pecsok, R. L. *Physicochemical Applications of Gas Chromatography*; Wiley: New York, 1978.
(2) Aspler, J. S. "*Theory and Applications of Inverse GC*". In *Pyrolysis and GC in Polymer Analysis*; Liebman, S. A., Levy, E. J., Eds.; Chromarographic Science Series; Dekker: New York, 1985; Vol. 29, Chapter IX.
(3) Lipson, J. E. G.; Guillet, J. E. "*Study of Structure and Interactions in Polymers by Inverse Gas Chromatography*". In *Developments in Polymer Characterization-3*; Dawkins, J. V., Ed.; Applied Science: Essex, England, 1982.
(4) Senich, G. A. *Polym. Prepr. (Am. Chem. Soc., Div. Polym. Chem.)* **1981**, *22*, 343.
(5) Braun, J. M.; Poos, S.; Guillet, J. E. *J. Polym. Sci., Polym. Lett. Ed.* **1976**, *14*, 257.
(6) Miltz, J. *Polymer* **1986**, *27*, 105.
(7) Tait, P. J. T.; Abushihada, A. M. *J. Chromatogr. Sci.* **1979**, *17*, 219.
(8) Kong, J. M.; Hawkes, S. J. *Macromolecules* **1975**, *8*, 148.
(9) Millen, W.; Hawkes, S. J. *J. Chromatogr. Sci.* **1977**, *15*, 148.
(10) Galin, M.; Rupprecht, M. C. *Polymer* **1978**, *19*, 506.
(11) Senich, G. A. Proc. *IUPAC, I.U.P.A.C., Makromol. Symp., 28th* **1982**, *28*, 1970.
(12) Kolk, J. F. M.; Matulewicz, E. R. A.; Moulijn, J. A. *J. Chromatogr. Sci.* **1978**, *11*, 160.
(13) Vidal-Madjor, C.; Guiochon, G. *J. Chromatogr.* **1977**, *61*, 142.
(14) Boniface, H. A.; Ruthven, D. M. *Chem. Eng. Sci.* **1985**, *40*, 1401.
(15) Van Deemter, J. J.; Zuderweg, F. J.; Klinkenberg, A. *Chem. Eng. Sci.* **1956**, *5*, 271.
(16) Giddings, J. C. *J. Chromatogr.* **1961**, *5*, 61.
(17) Giddings, J. C. *Anal. Chem.* **1963**, *35*, 439.
(18) Munk, P.; Card, T. W.; Hattam, P.; El-Hibri, M. J.; Al-Saigh, Z. Y. *Macromolecules* **1987**, *20*, 1278.
(19) Giddings, J. C. *J. Chromatogr.* **1961**, *5*, 49.
(20) McQuarrie, M. *J. Chem. Phys.* **1963**, *38*, 437.
(21) Kucera, E. *J.* Chromatogr. **1965**, *19*, 237.
(22) Kubin, M. *Collect. Czech. Chem. Commun.* **1965**, *30*, 1104.
(23) Vink, H. *J. Chromatogr.* **1965**, *20*, 305.
(24) Kaminskii, S. F.; Timasher, S. F.; Tunitskii, N. N. *J. Phys. Chem.* **1965**, *39*, 1354.
(25) Grubner, O.; Ralek, M.; Zikanova, A. *Collect. Czech. Chem. Commun.* **1966**, *31*, 852.
(26) Grubner, O. *Adv. Chromatogr. (N.Y.)* **1968**, *6*, 173.
(27) Grushka, E. *J. Phys. Chem.* **1972**, *76*, 2586.
(28) Anderson, D. J.; Walters, R. R. *J. Chromatogr. Sci.* **1984**, *22*, 353.
(29) Goedert, M.; Guiochon, G. *J. Chromatogr. Sci.* **1973**, *11*, 326.
(30) Chesler, S. N.; Cram, S. P. *Anal. Chem.* **1971**, *43*, 1922.
(31) Radeke, K. H. *Ind. Eng. Chem. Fundam.* **1981**, *20*, 302.
(32) Grushka, E.; Myers, M. N.; Schettler, P. D.; Giddings, J. C. *Anal. Chem.* **1969**, *41*, 889.
(33) Petitclerc, T.; Guiochon, G. *J. Chromatogr. Sci.* **1976**, *14*, 531.